G-2-5
Extended Abstracts of the 2012 International Conference on Solid State Devices and Materials, Kyoto, 2012, pp947-948

Dual Function of Charge Sensor: Charge Sensing and Gating

Tomohiro Kambara[1*], Tetsuo Kodera[1, 2, 3], Shunri Oda[1, 2]

[1] Quantum Nanoelectronics Research Center, Tokyo Institute of Technology,
2-12-1 O-okayama, Megro-ku, Tokyo 152-8550, Japan
[2] Institute for Nano Quantum Information Electronics, The Univ. of Tokyo, 4-6-1
Komaba, Meguro-ku, Tokyo 153-8505 Japan
[3] PRESTO, Japan Science and Technology Agency (JST), Kawaguchi, Saitama, Japan
*Phone: +81-3-5734-2542, Fax: +81-3-5734-2542, E-mail: kambara@neo.pe.titech.ac.jp

1. Introduction

Single electron spin is a promising candidate for solid-state quantum bit (qubit) because of its long coherence time [1,2]. Double quantum dots (DQDs) in various materials are studied to achieve the electron spin qubits [3]. Manipulation of electron spins in GaAs has already been reported [4–6]. However, the coherence time is limited because of hyperfine interaction [7]. On the other hand, electron spins in Si are expected to have a longer coherence time since there are almost no nuclear spins. The lifetimes of single electron spins in Si have recently been measured to be more than seconds [8]. A detection of single charge transition is necessary to read out electron states after control of the spins in DQDs. Single electron transistors or quantum point contacts are usually used as a charge sensor (CS) for the detection [9,10]. However, using CSs to each DQD needs a large space. Such large structure for qubits has a problem with integration to achieve quantum computer. Therefore, technological development of CSs which have multifunction not only of detecting charge transition of the DQDs but also of gating for DQDs is required.

In this work, we report the charge sensing and gating measurement of CSs. Charge transitions in a lithographically defined DQD are detected by a differential conductance of the integrated CS. The CS works also as a gate electrode for the DQD by applying negative voltages to both source and drain electrodes of the CS. In addition, the applied voltages of the CS have an additional advantage of modifying its own threshold voltage. These results suggest that the important technology for the integration of QDs is developed.

2. Device structure

The device structure we measured is shown in Fig. 1(a). Si DQD, CS and gates are fabricated by electron beam lithography, dry etching and thermal oxidation. The gates are used for controlling the electrochemical potential of each QD and modifying tunnel rates through each potential barrier. Constricted regions, controlled to be around 10 nm width, by the oxidation after dry etching, work as potential barrier for the DQD and CS. Back gate (BG) is used to induce 2-dimensional electron gas (2DEG) at the lower Si/SiO_2 interface in the silicon-on-insulator (SOI) layer. BG acts like a gate of metal-oxide-semiconductor field-effect transistor (MOSFET) structure.

Figure 1(b) shows a scanning electron microscopy (SEM) image of sample A. DQD and CS are schematically indicated by ovals. The thickness of the SOI layer is 30 nm, and that of the buried-oxide layer is 145 nm.

3. Results and discussion

Figure 2(a) shows a charge stability diagram of the DQD measured at 4.2 K. White dashed lines in Fig. 2(a) are detected lines of a charge transition by the CS shown in Fig. 2(b). Large current flows in the points of intersection of the dashed lines. The points indicate triple points which are typical characteristics of DQDs coupled in series. The charge transitions are successfully sensed by the integrated CS as shown in Fig. 2(b).

We applied the voltages to the source electrodes (V_{sCS}) and drain electrodes (V_{dCS}) of the CS in sample B [Fig. 3(a)]. Figure 3(b) shows measured differential conductance traces of the DQD as a function of the right gate voltage (V_{gr}). Here, from top to bottom V_{sCS} is increased from -1.5 V to -1.0 V in 0.05V steps. The change of the CS potential shifts Coulomb oscillation peaks of the DQD. Therefore, we successfully demonstrate that the CS works as another gate for the DQD.

Figure 3 (c) shows I_{dCS}-V_{sCS} characteristics, where I_{dCS} is a current through the CS. Switching characteristics of MOSFET with Coulomb oscillations are observed. By a voltage difference between the back gate voltage (V_{bg}) and V_{sCS}, an effective back gate voltage for the CS ($V_{effbg} = V_{bg} – V_{sCS}$) is determined. The V_{effbg} is shown at upper axis in Fig. 3(c). V_{effbg} only modulates a charge density of the CS. This result suggests that we can set working voltages of the DQD and the CS independently.

Figure 3(d) shows measured differential conductance traces of the CS as a function of V_{effbg}. Coulomb oscillations are observed and shifted slightly with decreasing V_{gr}. The electrochemical potential of the DQD is modified by V_{gr} and V_{sCS} while that of the CS is almost fixed against V_{gr}. V_{effbg} modulates the potential of the CS effectively, while the modulated CS works as a gate for the DQD, which is shown in Fig. 3 (b).

A matching of the working voltages for single charge transition of QDs and charge sensing by CSs is very important to investigate properties of QDs. The gating function of the CS can modify the potentials of the DQD and itself to match the working voltages. Dual function of the CS is a useful and important technique for flexible measurements in various QD devices.

4. Conclusions

We detected the charge transitions of the lithographically defined DQD by the integrated CS. The CS also works as a gate for the DQD with the voltages to the source and drain. Those voltages also shift its own threshold voltage. We obtained the technique of charge sensing and gating of the DQD with one CS.

Acknowledgements

This work was financially supported by KAKENHI (22246040, 24102703), JST-PRESTO, Yazaki Memorial Foundation for Science and Technology, and Project for Developing Innovation Systems of the Ministry of Education, Culture, Sports, Science and Technology (MEXT) and Global COE Program, "Photonics Integration-Core Electronics", MEXT, Japan. The devices were fabricated using EB-lithography facilities at QNERC-TIT.

References

[1] D. Loss and D. P. DiVincenzo, Phys. Rev. A **57** (1998) 120.
[2] J. M. Elzerman, *et al*., Nature **430** (2004) 431.
[3] D. P. DiVincenzo, Fortschr. Phys. **48** (2000) 771.
[4] R. Petta, *et al*. Science **309** (2005) 2180.
[5] F. H. L. Koppens, *et al*. Nature **442** (2006) 766.
[6] R. Brunner, *et al*. Phys. Rev. Lett. **107**, (20 11) 146801.
[7] A. Khaetskii, *et al*. Phys. Rev. B **67** (2003) 195329.
[8] Tyryshkin, A.M. *et al*. Nat. Mater. **10** (2011) 143-147.
[9] K. Horibe, *et al*. J. Appl. Phys. **111** (2012) 093715.
[10] M. G. Borselli, *et al*. Appl. Phys. Lett. **99** (2011) 063109.

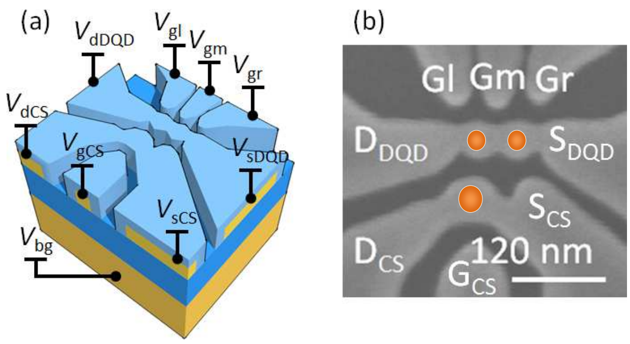

Fig. 1 (a) Schematic structure of sample A. DQD, CS and gates are covered with thermal-oxidized SiO_2 and the buried oxide. (b) Scanning electron microscopy (SEM) image of the sample. The DQD and CS are schematically indicated by ovals.

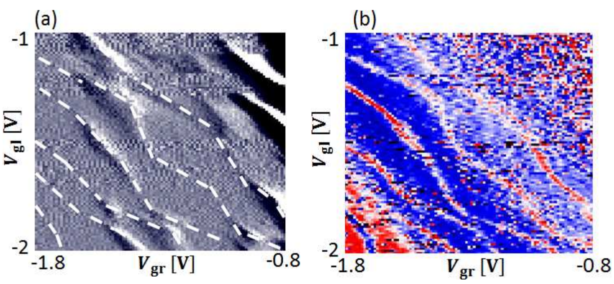

Fig. 2 (a) Charge stability diagram of the DQD. White dashed lines show the same lines in (b) obtained by CS. (b) Differential conductance of the CS. The charge detection lines are clearly observed.

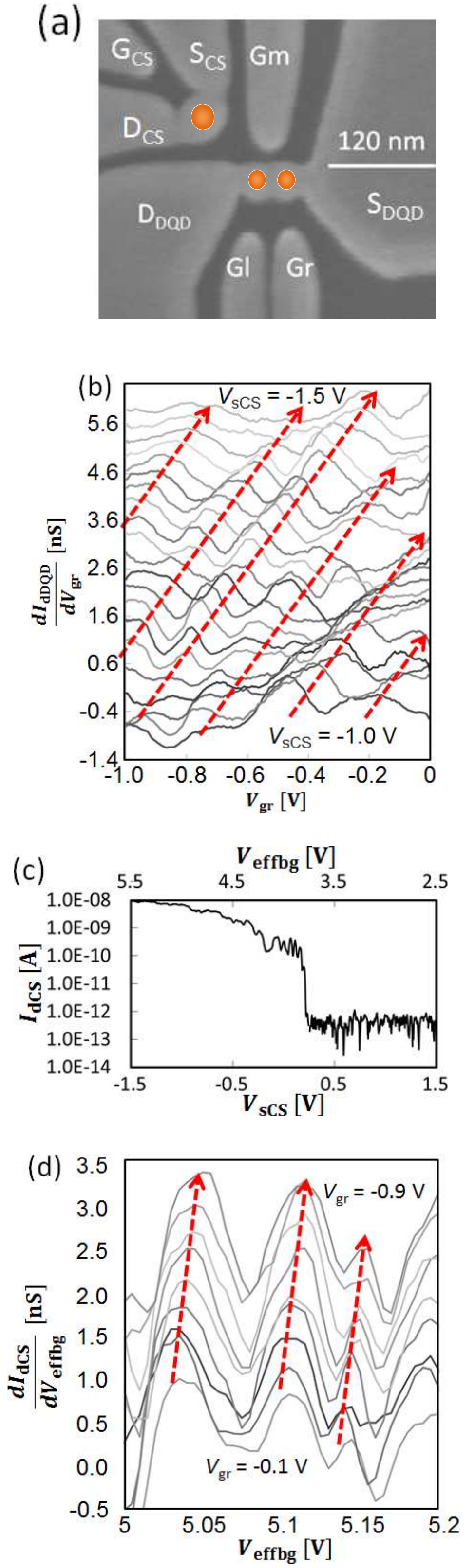

Fig. 3 (a) SEM image of sample B. (b) Measured differential conductance traces of the DQD for V_{sCS} between -1.0 V (bottom trace) and -1.5 V (top trace). The traces have been given an offset for clarity. Red dashed arrows are used for eye-guide. (c) I_{dCS}-V_{sCS} characteristics. V_{effbg} (= V_{bg} – V_{sCS}) is shown at upper axis. (d) dI_{dCS}/dV_{effbg} as a function of V_{effbg}.